An exact result concerning the 1/f noise contribution to the large-angle error in CMB temperature and polarization maps

Martin Bucher, APC, Université Paris 7

CERN, 19 May 2016

Searching for B modes : sensitivities vs. Expected signal

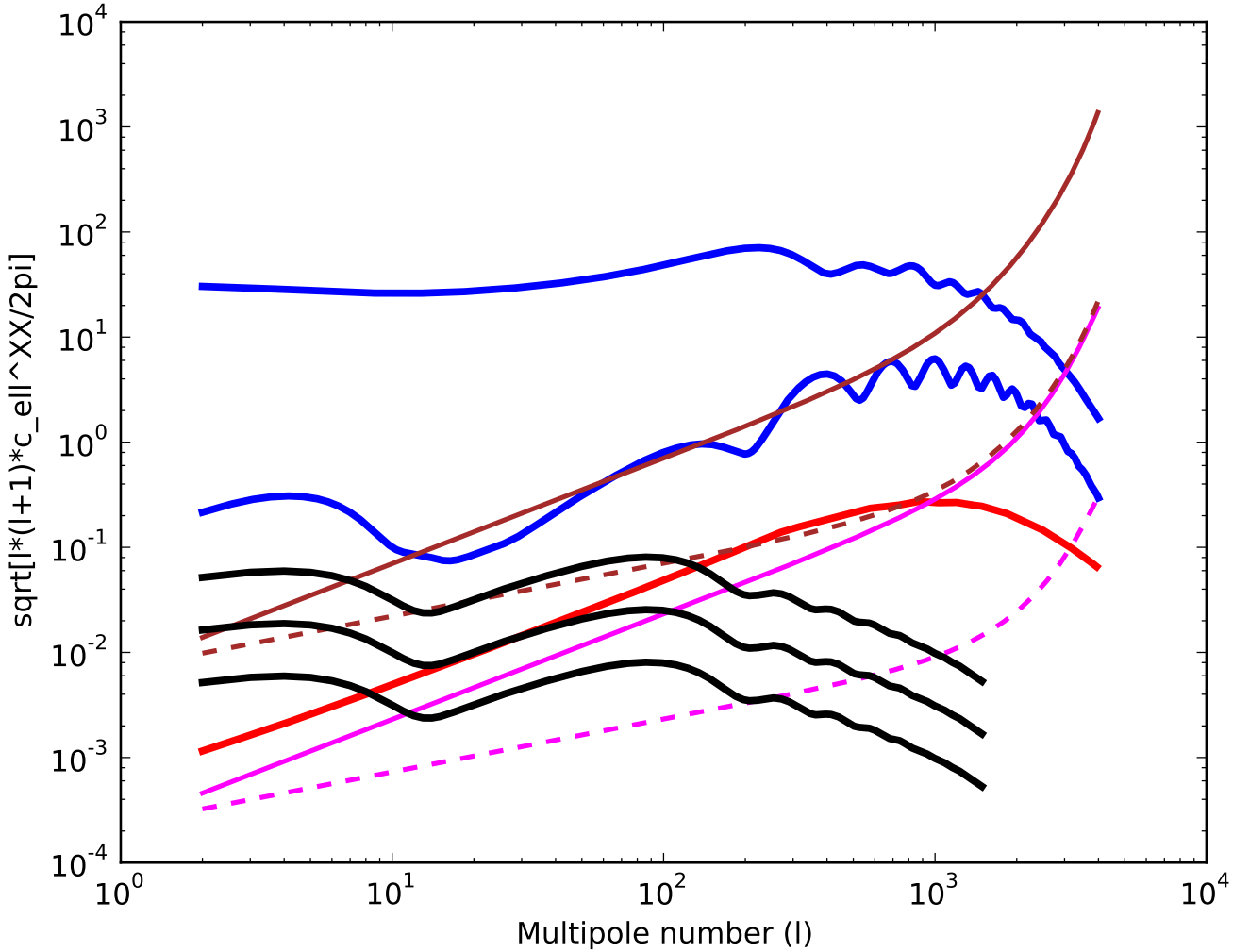

brown=planck ; magenta=COrE ; dashed = broad binning $\Delta\ell \approx \ell$, black=BB, ten for $r = 10^{-1}$, $r = 10^{-2}$, and $r = 10^{-3}$

Astronomy & Astrophysics manuscript no. LowEll
Wednesday 11th May, 2016

Planck 2016 intermediate results. XLVI. Reduction of large-scale systematic effects in HFI polarization maps and estimation of the reionization optical depth

Planck Collaboration: N. Aghanim[53], M. Ashdown[63,6], J. Aumont[53], C. Baccigalupi[75], M. Ballardini[29,45,48], A. J. Banday[85,9], R. B. Barreiro[58], N. Bartolo[28,59], S. Basak[75], R. Battye[61], K. Benabed[54,84], J.-P. Bernard[85,9], M. Bersanelli[32,46], P. Bielewicz[72,9,75], J. J. Bock[60,10], A. Bonaldi[61], L. Bonavera[16], J. R. Bond[8], J. Borrill[12,81], F. R. Bouchet[54,79], F. Boulanger[53], M. Bucher[1], C. Burigana[45,30,48], R. C. Butler[45], E. Calabrese[82], J.-F. Cardoso[66,1,54], J. Carron[21], A. Challinor[55,63,11], H. C. Chiang[23,7], L. P. L. Colombo[19,60], C. Combet[67], B. Comis[67], A. Coulais[65], B. P. Crill[60,10], A. Curto[58,6,63], F. Cuttaia[45], R. J. Davis[61], P. de Bernardis[31], A. de Rosa[45], G. de Zotti[42,75], J. Delabrouille[1], J.-M. Delouis[54,84], E. Di Valentino[54,79], C. Dickinson[61], J. M. Diego[58], O. Doré[60,10], M. Douspis[53], A. Ducout[54,52], X. Dupac[36], G. Efstathiou[55], F. Elsner[20,54,84], T. A. Enßlin[70], H. K. Eriksen[56], E. Falgarone[65], Y. Fantaye[34], F. Finelli[45,48], F. Forastieri[30,49], M. Frailis[44], A. A. Fraisse[23], E. Franceschi[45], A. Frolov[78], S. Galeotta[44], S. Galli[62], K. Ganga[1], R. T. Génova-Santos[57,15], M. Gerbino[83,74,31], T. Ghosh[53], J. González-Nuevo[16,58], K. M. Górski[60,87], S. Gratton[63,55], A. Gruppuso[45,48], J. E. Gudmundsson[83,74,23], F. K. Hansen[56], G. Helou[10], S. Henrot-Versillé[64], D. Herranz[58], E. Hivon[54,84], Z. Huang[8], S. Ilić[85,9,5], A. H. Jaffe[52], W. C. Jones[23], E. Keihänen[22], R. Keskitalo[12], T. S. Kisner[69], L. Knox[25], N. Krachmalnicoff[32], M. Kunz[14,53,2], H. Kurki-Suonio[22,41], G. Lagache[4,53], J.-M. Lamarre[65], M. Langer[53], A. Lasenby[6,63], M. Lattanzi[30,49], C. R. Lawrence[60], M. Le Jeune[1], J. P. Leahy[61], F. Levrier[65], M. Liguori[28,59], P. B. Lilje[56], M. López-Caniego[36], Y.-Z. Ma[61,76], J. F. Macías-Pérez[67], G. Maggio[44], A. Mangilli[53,64], M. Maris[44], P. G. Martin[8], E. Martínez-González[58], S. Matarrese[28,59,38], N. Mauri[48], J. D. McEwen[71], P. R. Meinhold[26], A. Melchiorri[31,50], A. Mennella[32,46], M. Migliaccio[55,63], M.-A. Miville-Deschênes[53,8], D. Molinari[30,45,49], A. Moneti[54], L. Montier[85,9], G. Morgante[45], A. Moss[77], S. Mottet[54,79], P. Naselsky[73,35], P. Natoli[30,3,49], C. A. Oxborrow[13], L. Pagano[31,50], D. Paoletti[45,48], B. Partridge[40], G. Patanchon[1], L. Patrizii[48], O. Perdereau[64], L. Perotto[67], V. Pettorino[39], F. Piacentini[31], S. Plaszczynski[64], L. Polastri[30,49], G. Polenta[3,43], J.-L. Puget[53 *], J. P. Rachen[17,70], B. Racine[1], M. Reinecke[70], M. Remazeilles[61,53,1], A. Renzi[34,51], G. Rocha[60,10], M. Rossetti[32,46], G. Roudier[1,65,60], J. A. Rubiño-Martín[57,15], B. Ruiz-Granados[86], L. Salvati[31], M. Sandri[45], M. Savelainen[22,41], D. Scott[18], G. Sirri[48], R. Sunyaev[70,80], A.-S. Suur-Uski[22,41], J. A. Tauber[37], M. Tenti[47], L. Toffolatti[16,58,45], M. Tomasi[32,46], M. Tristram[64], T. Trombetti[45,30], J. Valiviita[22,41], F. Van Tent[68], L. Vibert[53], P. Vielva[58], F. Villa[45], N. Vittorio[33], B. D. Wandelt[54,84,27], R. Watson[61], I. K. Wehus[60,56], M. White[24], A. Zacchei[44], and A. Zonca[26]

(Affiliations can be found after the references)

Wednesday 11th May, 2016

ABSTRACT

This paper describes the identification, modelling, and removal of previously unexplained systematic effects in the polarization data of the *Planck* High Frequency Instrument (HFI) on large angular scales, including new mapmaking and calibration procedures, new and more complete end-to-end simulations, and a set of robust internal consistency checks on the resulting maps. These maps, at 100, 143, 217, and 353 GHz, are early versions of those that will be released in final form later in 2016. The improvements allow us to determine the cosmic reionization optical depth τ using, for the first time, the low-multipole EE data from HFI, reducing significantly the central value and uncertainty, and hence the upper limit. Two different likelihood procedures are used to constrain τ from two estimators of the CMB E- and B-mode angular power spectra at 100 and 143 GHz, after debiasing the spectra from a small remaining systematic contamination. These all give fully consistent results. A further consistency test is performed using cross-correlations derived from the Low Frequency Instrument maps of the *Planck* 2015 data release and the new HFI data. For this purpose, end-to-end analyses of systematic effects from the two instruments are used to demonstrate the near independence of their dominant systematic error residuals. The tightest result comes from the HFI-based τ posterior distribution using the maximum likelihood power spectrum estimator, giving a value 0.055 ± 0.009. In a companion paper these results are discussed in the context of the best-fit *Planck* ΛCDM cosmological model and recent models of reionization.

Key words. Cosmology: observations – dark ages, reionization, first stars – Cosmic background radiation – Space vehicles: instruments – Instrumentation: detectors

1. Introduction

The E-mode polarization signal of the cosmic microwave background (CMB) at multipoles less than 15 is sensitive to the value of the Thomson scattering optical depth τ. In polarization at large angular scales, the extra signal generated by reionization dominates over the signal from recombination. CMB polarization measurements thus provide an important constraint on models of early galaxy evolution and star formation, providing the integrated optical depth of the entire history of reionization, which is complementary information to the lower limit on the redshift of full reionization provided by Lyman-α absorption in the spectra of high redshift objects (see Dijkstra 2014; Mashian et al. 2016; Robertson et al. 2015; Bouwens et al. 2015; Zitrin et al. 2015, for recent results and reviews). The reionization parameter τ is difficult to constrain with CMB temperature measurements alone, as the TT power spectrum depends on the combination $A_s e^{-2\tau}$, and τ is degenerate with A_s, the amplitude of the initial cosmological scalar perturbations.

The B-mode polarization signal at low multipoles is created by the scattering of primordial tensor anisotropies in the CMB by reionized matter. This signal scales roughly as τ^2. The value of τ is thus also important for experiments constraining the tensor-to-scalar ratio, r, using the reionization peak of the B modes.

Due to the large angular scale of the signals, τ has been measured only in full-sky measurements made from space.

*Corresponding author: J. L. Puget,
jean-loup.puget@ias.u-psud.fr

Detector noise PS from Planck

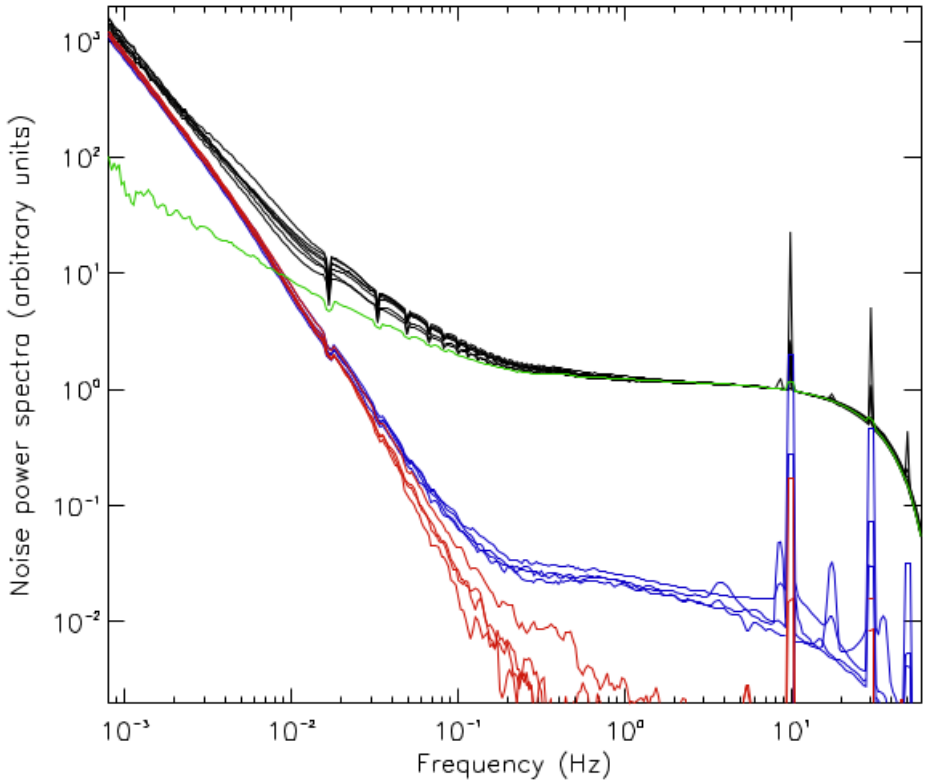

Fig. 2. Noise cross-power spectra of the 143-GHz bolometers, with the unpolarized spider-web bolometers (SWBs) in red and the polarization-sensitive bolometers (PSBs) in blue. The low-level correlated white noise component of the PSB noise is associated with common glitches below the detection threshold. Auto-spectra are shown in black. The uncorrelated noise is in green.

$\nu_{knee} = 200 mHz.$

Standard Ansatz for detector noise

We assume Gaussian stationary noise completely characterized by a power spectrum

$$\langle n(\nu)\, n(\nu')\rangle = N(\nu)\delta(\nu - \nu'), \tag{1}$$

and additionally the Ansatz

$$N(\nu) = N_{white}\left(1 + \left(\frac{\nu_{knee}}{\nu}\right)^{\alpha}\right]. \tag{2}$$

Typically, $1 \lesssim \alpha \lesssim 2$ and $\nu_{knee} \approx 200$ *mHz* for Planck but has been observed as small as 10 *mHz* in the laboratory. However, the Planck detectors tested in the lab showed comparable performance, and it is not fully understood why the performance in space was so much poorer.

Lesson : You should be worried.

The map making equation (easy to write, harder to solve for big maps)

The underlying (approximate) statistical model

$$\mathbf{d} = \mathbf{A}\,\mathbf{m} + \mathbf{n} \tag{3}$$

$\mathbf{d} \equiv$ (vector of data taken)

$\mathbf{m} \equiv$ (true sky map)

$\mathbf{A} \equiv$ (pointing matrix)

$\mathbf{n} \equiv$ (noise vector)

$\mathbf{N} \equiv$ (detector noise covariance matrix)

The **maximum likelihood sky map** is given by

$$\mathbf{m}_{ML} = (\mathbf{A}^T\mathbf{N}^{-1}\mathbf{A})^{-1}(\mathbf{A}^T\mathbf{N}^{-1})\mathbf{d} \tag{4}$$

The curse of low frequency excess noise

- $1/f^{\alpha}$ noise means that we cannot make absolute measurements.
- The zero point is floating and provides no meaningful information.

Mathematically, the integral

$$N(t) = 2 \int_0^{\infty} d\nu \; N(\nu) \; \cos(2\pi\nu t) \tag{5}$$

diverges for $\alpha \geq 0$.

- Only differences of measurements taken between a short time span $t \lesssim {\nu_{knee}}^{-1}$ contribute meaningful information.

The curse of $1/f$ noise is not new

- In 1947 Dicke proposed switching between different points in the sky or between the sky and a cold source to eliminate $1/f$ noise in the microwave amplifiers/detector available at the time.
- COBE and WMAP had pairs of horns or telescope, respectively, and only the differences were used, so that the noise of the data stream was more or less "white". Planck LFI did more or less the same but with an artificial load. HEMTs must be switched at $\approx$ (few) kHz is order to control low frequency excess noise.
- Old map making is simple—essentially least squares—whereas modern map making would not be possible without fast computers. Implicit differencing in software replaces differences implemented in hardware.

The map making filter $N^{-1}(t)$

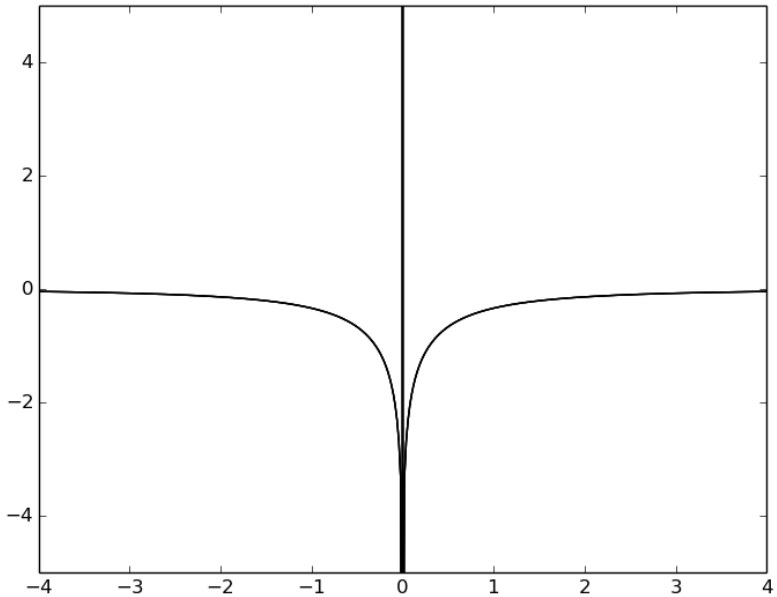

$$
\begin{aligned}
N^{-1}(t) &= 2\int_0^\infty d\nu\, N^{-1}(\nu)\, \cos(2\pi\nu t) \\
&= 2{N_{white}}^{-1}\int_0^\infty d\nu \left(\frac{\nu}{\nu+\nu_{knee}}\right) \cos(2\pi\nu t), \qquad (6)
\end{aligned}
$$

This is a high pass filter. The $\nu = 0$ is completely blocked. The constant offset and linear drifts are removed from the data stream because they carry no useful information.

Spin-precession family of scanning strategies

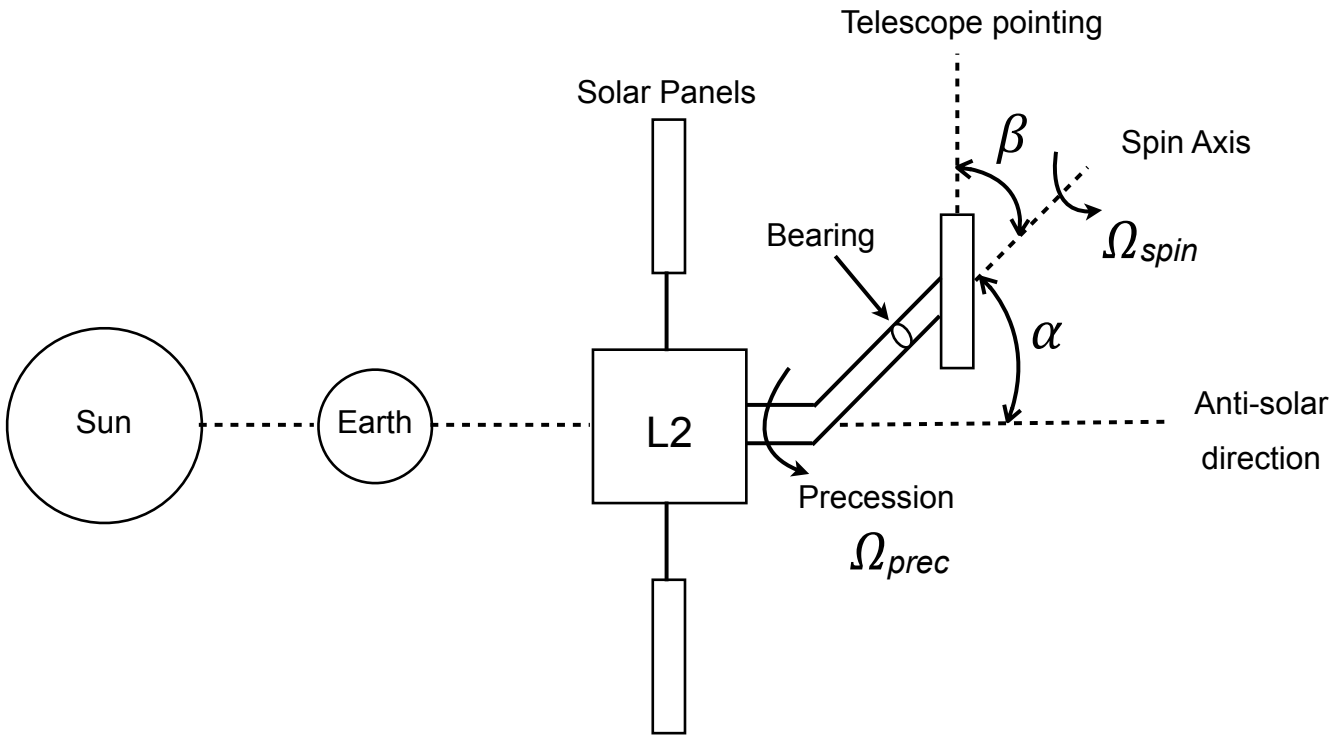

Pattern on sky

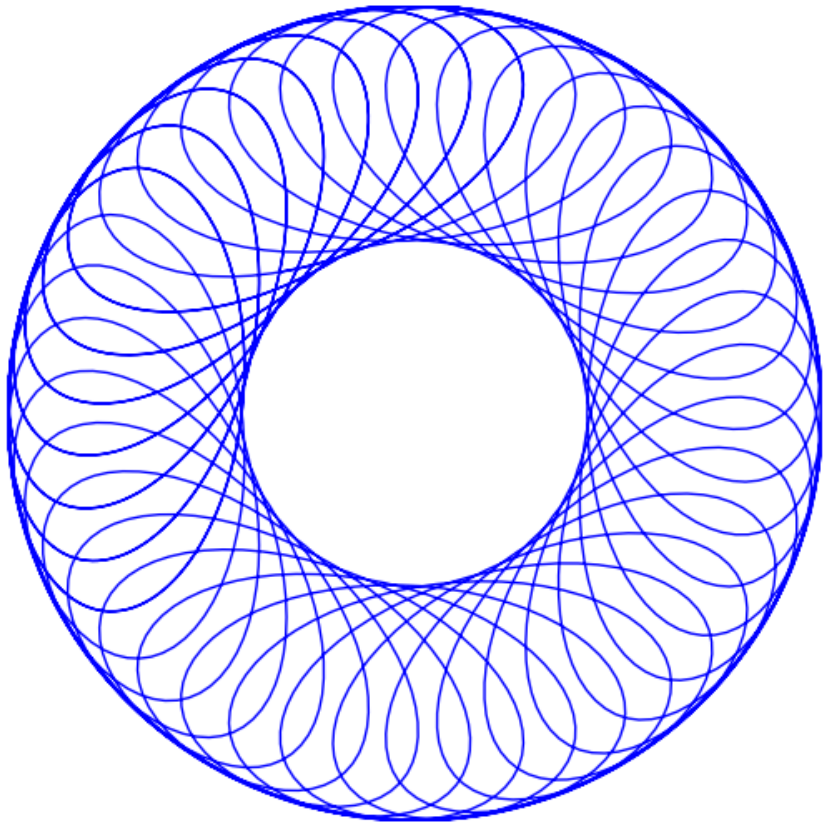

This pattern is centered on the ecliptic equator and precesses around over the course of the year.

Isotropic scans

- We assume that every pixel is scanned in exactly the same way in a manner isotropic under rotations about the pixel center and that the polarizer orientations have an isotropic distribution. (The latter assumption in fact can be relaxed.)
- Under these assumption, we can use functional analysis (the study of operators on infinite dimensional function spaces) rather than finite-dimensional linear algebra. The isotropy allows us to solve for the final map covariance matrix in terms of simple one-dimensional integrals.
- Does not apply exactly to most scan strategies, but many more cases can be studied and invaluable intuition can be gained.

Temperature case : solving the map covariance matrix for an isotropic scan

The operator

$$\mathcal{O} = (\mathbf{A}^T \mathbf{N}^{-1} \mathbf{A}) \tag{7}$$

is the map inverse noise matrix.
We may expand

$$\left(\mathbf{A}^T \mathbf{N}^{-1} \mathbf{A}\right)(\widehat{\Omega}, \widehat{\Omega}') \quad = (\mathcal{N}_{white})^{-1} \sum_{\ell=0}^{\infty} w_\ell^T \sum_{m=-\ell}^{+\ell} Y_{\ell m}(\widehat{\Omega})\, Y^*_{\ell m}(\widehat{\Omega}'), \tag{8}$$

and solve for the eigenvalue as follows

$$w_\ell^T \quad = \quad 1 - \sum_{(i)=1}^{n} f_{(i)} \int_{-\infty}^{+\infty} dt\ (2\nu_{knee})\ g(2\pi\nu_{knee}|t|)\ P_\ell\left(\cos[\theta_{(i)}(t)]\right) \tag{9}$$

Temperature case : boost factor

$$\beta = \text{spin opening radius (in degrees)}$$

$$\omega_{spin} = \frac{\nu_{spin}}{\nu_{knee}}$$

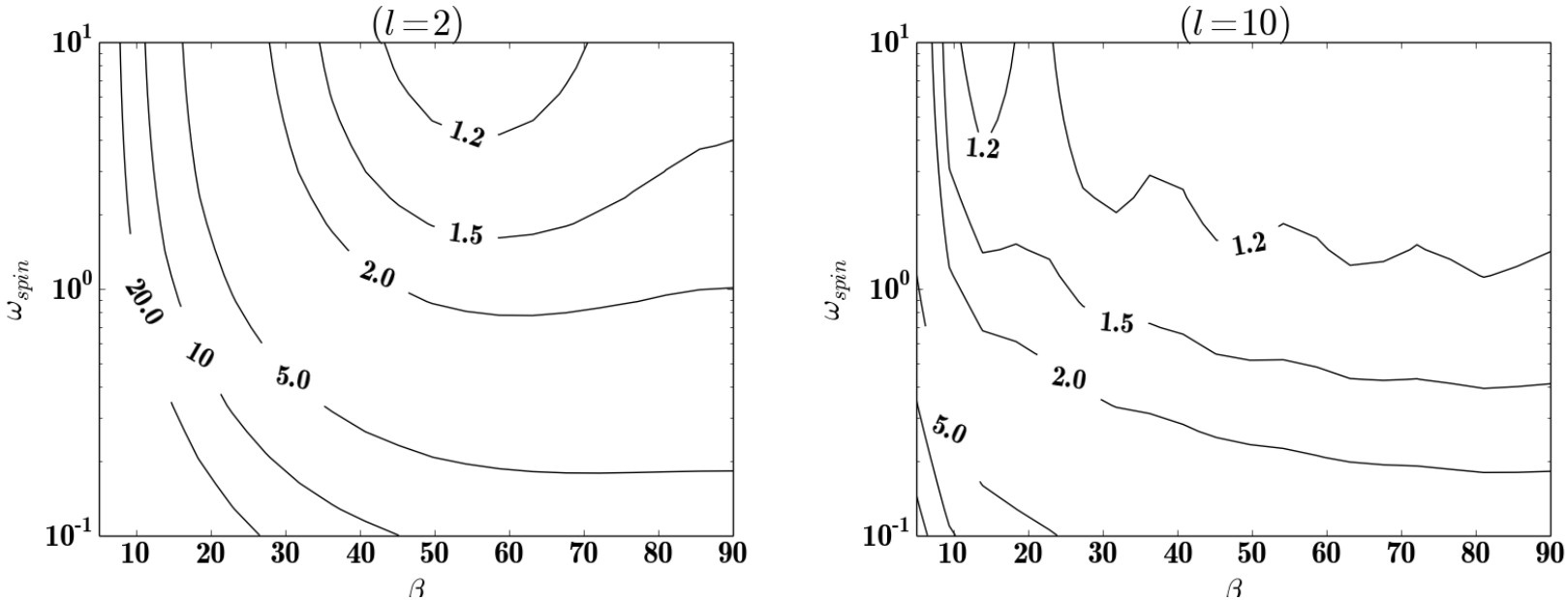

$$(\text{Boost factor})_\ell \equiv \frac{n_\ell(\text{white noise + 1/f}^\alpha \text{ noise})}{n_\ell(\text{white noise only})}$$

Comparing polarizations in presence of 1/f noise

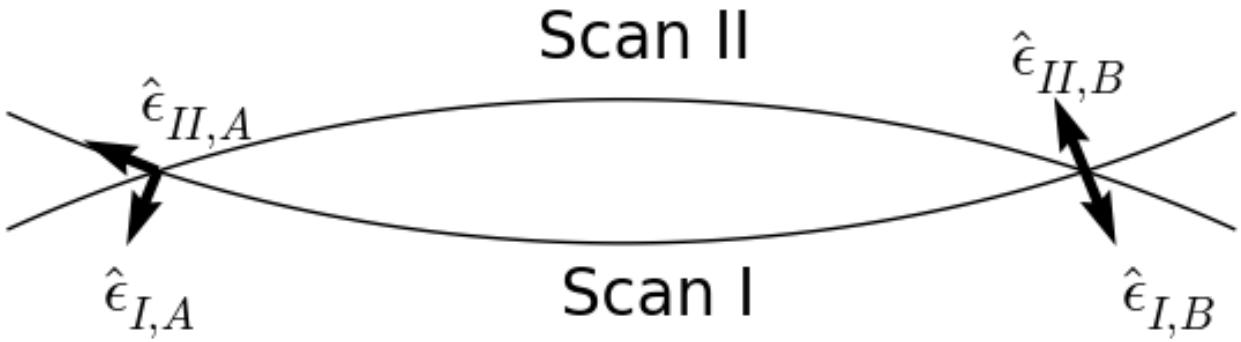

Polarization case : a bit messier but doable

The polarization measurements are modelled as follows :

$$T(t) = I(t) + \cos 2\xi(t)\ Q(t) + \sin 2\xi(t)\ U(t), \tag{10}$$

We obtain the eigenvalue/eigenfunction equation

$$\sum_{(i)} f_{(i)} \int_{-\pi}^{+\pi} \frac{d\bar{\phi}}{2\pi} \int_{-\infty}^{+\infty} dT\ g(T)\ \mathrm{Re}\left[\exp[-2i\bar{\phi}]\ \mathbf{E}_{j2}\Big(\theta_{(i)}(T, \bar{\phi}=0), \phi_{(i)}(T, \bar{\phi}=0)\Big)\right]$$
$$\mathbf{e}(T; +, \bar{\phi}=0)$$
$$= w_j^P \mathrm{Re}\left[\ \mathbf{E}_{j2}(N.P.) \cdot \mathbf{e}_{+,N.P.}\right]. \tag{11}$$

Final polarization result

$$
\begin{aligned}
w_j^P &= 1 - \sum_{(i)} f_{(i)} \int_{-\infty}^{+\infty} dT\, g(T) \int_{-\pi}^{+\pi} \frac{d\bar{\phi}}{2\pi} \frac{1}{Q_{j,2}(1)} \\
&\quad \times \mathrm{Re}\Bigg[\Big(\cos[2(\phi_{(i)} + \bar{\phi})]\, Q_{j,2}(\cos\theta_i(T)) + i \sin[2(\phi_{(i)} + \bar{\phi})]\, U_{j,2}(\cos\theta_{(i)}(T)) \Big) \\
&\qquad \times \exp\Big[-2i\{\bar{\phi} + \Delta\chi_{(i)}(T)\} \Big] \Bigg] \\
&= 1 - \sum_{(i)} f_{(i)} \int_{-\infty}^{+\infty} dT\, g(T) \frac{Q_{j,2}(\cos\theta_i(T)) + U_{j,2}(\cos\theta_i(T))}{2Q_{j,2}(1)} \\
&\quad \times \exp\Big[2i\{\phi_{(i)}(T) - \Delta\chi_{(i)}(T)\} \Big] \\
&= 1 - \sum_{(i)} f_{(i)} \int_{-\infty}^{+\infty} dT\, g(T) \frac{Q_{j,2}(\cos\theta_i(T)) + U_{j,2}(\cos\theta_i(T))}{2Q_{j,2}(1)} \\
&\quad \times \cos\Big[2\{\phi_{(i)}(T) - \Delta\chi_{(i)}(T)\} \Big]. \qquad (12)
\end{aligned}
$$

Polarization case : boost factor

These are results **without** a rotating half-wave plate.

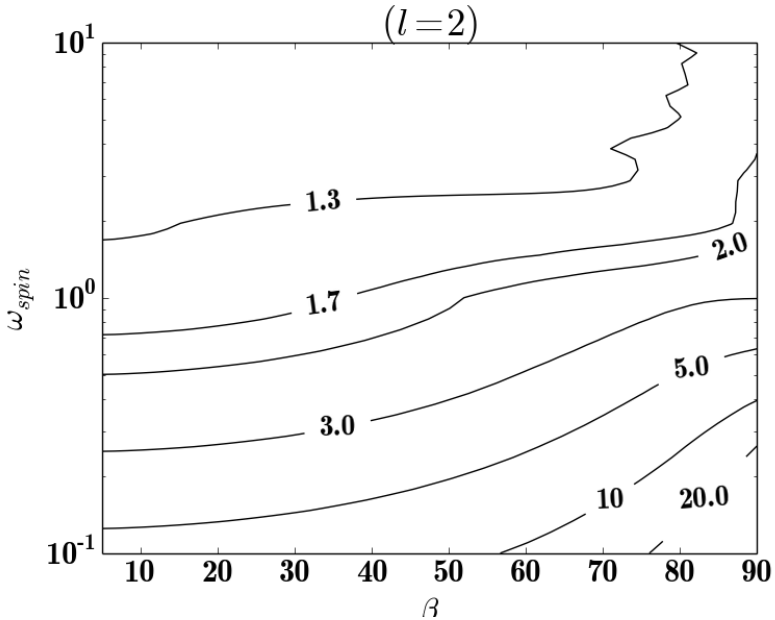

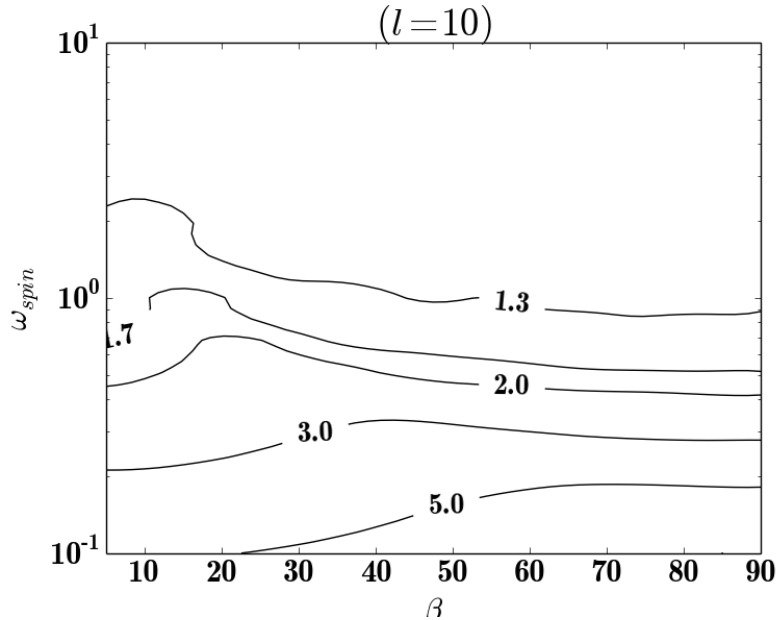

Polarization case : boost factor

These are results **with** a rotating half-wave plate.

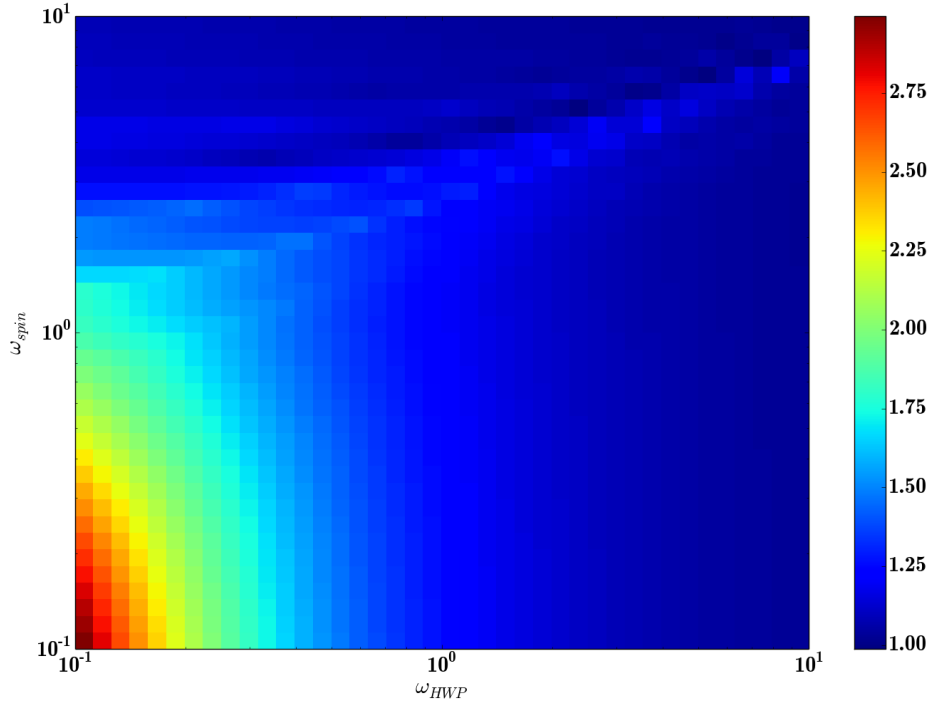

$$\ell = 2$$

Conclusions

- $1/f$ noise is a problem that can be important and could seriously compromise ultimate instrument performance. It is hard to predict level of 1/f noise in space.
- The map making equation (and this analysis) does not include a lot of possible complexity. Actual performance could be much worse than forecast. Actual performance cannot be better than forecast, contrary to what some people believe. There are no magic software solutions to gain information not present in the measurements themselves. The map making equation gives the ideal sky map given the data taken (subject to some assumptions).
- This work demonstrates that not everything is a Big Data/Supercomputer problem to be tackled with comprehensive "end-to-end" simulations. There is scope for simple models for accounting for systematic errors studied in isolation. Simple models provide intuition and allow many more cases to be analyzed.

An exact result concerning the $1/f$ noise contribution to the large-angle error in CMB temperature and polarization maps

Martin Bucher (Laboratoire APC, Université Paris 7/CNRS, Paris, France and Department of Mathematics, Statistics and Computer Science, University of KwaZulu-Natal, Durban, South Africa)

(Submitted on 26 Feb 2016 (v1), last revised 29 Feb 2016 (this version, v2))

We present an exact expression for the $1/f$ contribution to the noise of the CMB temperature and polarization maps for a survey in which the scan pattern is isotropic. The result for polarization applies likewise to surveys with and without a rotating half-wave plate. A representative range of survey parameters is explored and implications for the design and optimization of future surveys are discussed. These results are most directly applicable to space-based surveys, which afford considerable freedom in the choice of the scan pattern on the celestial sphere. We discuss the applicability of the methods developed here to analyzing past experiments and present some conclusions pertinent to the design of future experiments. The techniques developed here do not require that the excess low frequency noise have exactly the $1/f$ shape and readily generalize to other functional forms for the detector noise power spectrum. In the case of weakly anisotropic scanning patterns the techniques in this paper can be used to find a preconditioner for solving the map making equation efficiently using the conjugate gradient method.

Comments: 20 pages REVTEX, 7 figures, minor typos corrected

Subjects: **Instrumentation and Methods for Astrophysics (astro-ph.IM)**; Cosmology and Nongalactic Astrophysics (astro-ph.CO)

Cite as: **arXiv:1602.08274 [astro-ph.IM]**

(or **arXiv:1602.08274v2 [astro-ph.IM]** for this version)

Submission history

From: Martin Bucher [view email]

[v1] Fri, 26 Feb 2016 10:59:49 GMT (507kb,D)

[v2] Mon, 29 Feb 2016 02:04:15 GMT (508kb,D)